

AAS 09-390



**CLOSED-LOOP ONE-DIMENSIONAL CHARGED
RELATIVE MOTION EXPERIMENTS
SIMULATING CONSTRAINED ORBITAL MOTION**

Carl R. Seubert and Hanspeter Schaub

**AAS/AIAA Astrodynamics Specialist
Conference**

Pittsburgh, PA

August 9-13, 2009

AAS Publications Office, P.O. Box 28130, San Diego, CA 92198

CLOSED-LOOP ONE-DIMENSIONAL CHARGED RELATIVE MOTION EXPERIMENTS SIMULATING CONSTRAINED ORBITAL MOTION

Carl R. Seubert* and Hanspeter Schaub†

Coulomb spacecraft actively control their potential through continuous charge emission to generate inter-spacecraft electrostatic forces. Modeling the complex induced charge effects and coupling with the plasma environment is very challenging. This paper presents charged relative motion experiments demonstrating how active charge feedback control tests can be performed in a terrestrial environment without resorting to expensive vacuum or plasma chambers. The non-conducting test bed is able to levitate a conducting sphere with only milli-Newton level disturbance forces. The relative motion is achieved by having one charged sphere stationary and one charged sphere floating on the track. Charge control is provided through an external potential source connected to the spheres through a small conducting wire. The one-dimensional (1-D) test track can mimic the constrained motion along the orbit radial, along-track, or out-of-plane direction. These dynamical systems are replicated with the test track by either leveling it, or adding a small tilt to bias the relative motion in one direction. Experimental results illustrate the performance of a simple charge feedback control for these orbital scenarios.

INTRODUCTION

There are many advantages to spacecraft flying in formation, such as being used for scientific and exploratory missions, including the generation of large sensor baselines for high resolution interferometry. Other advantages include the use of smaller and lighter spacecraft, system redundancy, and distributed network space systems. The technical and logistical challenges of formation flight are being overcome with numerous successful missions and many concepts in planning.^{1,2}

Close spacecraft formations on the order of dozens of meters present particular mission challenges, including accurate relative position sensing and frequent micro-Newton-level control to perform relative motion maneuvers. Other close proximity aspects to be further investigated are autonomous rendezvous and docking, as well as the deployment and the use of tethered spacecraft systems. Further, if conventional inertial thrusters such as chemical or electric propulsion techniques are used, then care must be taken at these separation distances to ensure exhaust plumes do not impinge on the other craft and damage sensors and structural components. Coulomb (electrostatic) thrust is a novel method to control the separation distances of spacecraft flying in close formation and resolves plume impingement concerns. Another advantage of Coulomb thrust is that it offers separation distance control for very low power consumption (Watt levels) and very low propellant mass (ejects electrons or low-mass ions).^{3,4}

*Graduate Research Assistant, Aerospace Engineering Sciences Department, University of Colorado, Boulder, CO. AIAA student member, AAS student member

†Associate Professor, H. Joseph Smead Fellow, Aerospace Engineering Sciences Department, University of Colorado, Boulder, CO. AIAA Associate Fellow, AAS member

Due to the natural shielding effects from the space plasma environment, Coulomb control is best utilized for separation distances less than 100 meters and formation altitudes of geostationary Earth orbit (GEO) and above.³ Experiments on the Coulomb testbed are performed in a standard atmospheric environment and presently do not investigate space plasma interaction. Interestingly, current testing indicates there is interaction with the testbed's charged spheres and the atmosphere. This is an area requiring further examination and is not covered in this paper.

Orbital missions such as SCATHA and ATS-6 have shown that spacecraft charging naturally occurs as a result of interaction with the local plasma environment.^{5,6} A spacecraft in GEO can naturally charge to kilovolt level potentials.^{7,8} Natural spacecraft charging can be safely prevented and overcome as shown with missions such as Equator-S, CLUSTER and SPEAR 1.^{9,10,11} ESA CLUSTER spacecraft utilize very precise potential control by emitting indium ions at 5-9 keV energies from a liquid metal source.¹¹ The Coulomb thrust concept described in this paper utilizes this proven space technology and does not require the high precision charge control demonstrated by the CLUSTER mission.¹² Furthermore, it is the absolute potential of the craft that produces the Coulomb force; consequently, another advantage of the concept is that natural charge levels can be utilized and then modified as necessary to perform an operational maneuver.

The proposed NASA Goddard Stellar Imager¹³ and the NASA JPL study on the proposed Terrestrial Planet Finder¹⁴ are two missions that could potentially utilize Coulomb thrust techniques for formation control. Each of these proposed missions intends to use a formation of spacecraft to create a sensor baseline in the kilometer range. Another application of the Coulomb thrust concept that is being investigated is the deflection of near Earth objects.¹⁵

This paper details the demonstration of 1-D feedback control of a craft using Coulomb forces. An example of a simple two spacecraft formation using Coulomb forces for separation distance control is shown in Figure 1. This testbed allows experiments that mimic simplified two-craft orbit scenarios and expands the future capabilities of spacecraft Coulomb control.

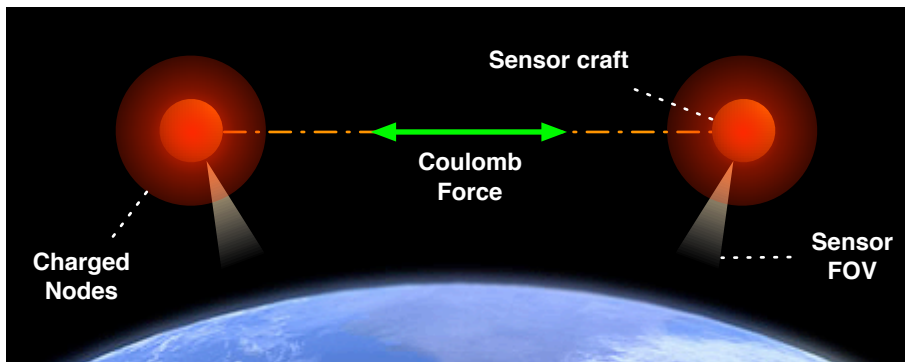


Figure 1 Two sensor nodes using Coulomb forces to provide the necessary formation separation distance

Terrestrial testbeds have been developed to explore the techniques and control of spacecraft formations. These include JPL's Formation Control Testbed¹⁶ and NASA Marshall Space Flight Center flat floor testbed.¹⁷ These testbeds provide a flat, near frictionless operating surface that allows terrestrial relative motion experiments using linear air-bearing pads or similar. The intent of these testbeds is to test and verify hardware and operational subsystems.

The motion experiments conducted on traditional testbeds such as these are performed with

well-known dynamics and typically with conventional thrusters with force capabilities magnitudes greater than the Coulomb thrust technique. Consequently, there are numerous challenges to performing terrestrial motion experiments with the Coulomb thrust concept. The control forces are tens of milli-newtons or less,¹⁸ requiring disturbances to be even smaller in magnitude. Coulomb force modeling is currently simplified by excluding interactions with the atmosphere. The model can be improved through further development and testbed verification.

The Coulomb testbed in the Autonomous Vehicle Systems (AVS) laboratory at the University of Colorado at Boulder is developed specifically to demonstrate the actuation of vehicles under the control of Coulomb forces. This low-cost 1-D version allows motion studies in which control forces dominate disturbances. It also allows the investigation of electrostatic interactions and induced effects, application of control algorithms, and advances the knowledge and implementation of hardware technologies. Future testbed generations will evolve to a two dimensional (2-D) platform and ultimately incorporate environmental modeling such as vacuum operation.

The Coulomb testbed does not simulate or demonstrate motion in a space environment. It does allow tests to be performed that mimic orbit-similar scenarios through the implementation of feedback control. This paper presents the results of tests that are similar to the control of two spacecraft operating in three linearly constrained configurations: orbit radial, along-track and out-of-plane. The testbed, displayed in figure 2, shows the stationary charged sphere and the cart with charged sphere on the track. The vehicle's position is manipulated by controlling the charge level of the spheres. The orbit configurations are mimicked by tilting the track to induce a bias gravitational force similar to a gravity gradient force in orbit.

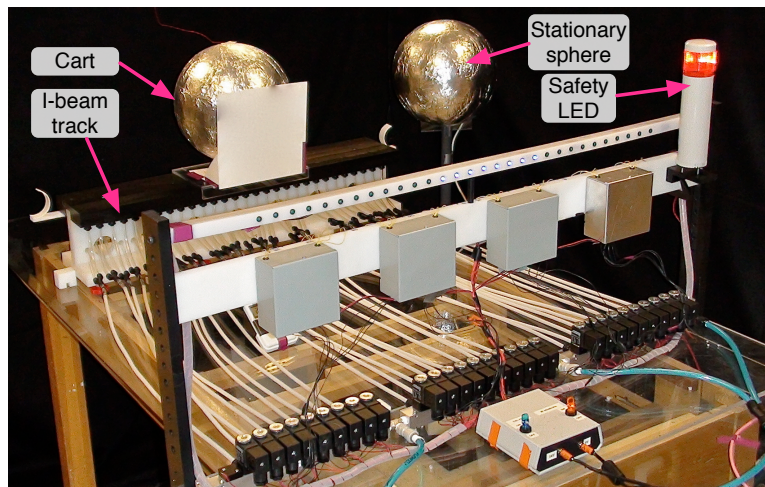


Figure 2. Testbed configuration used for feedback control on cart position with Coulomb forces.

The previously published achievements of the Coulomb testbed are simple attractive and repulsive tests on the track.¹⁸ The disturbances in these results are large, however Coulomb actuation is successfully demonstrated. This early work has since led to a reduction in disturbances and the implementation of feedback control and autonomous cart motion. This paper documents the improvements made to the testbed to yield lower disturbance forces. Further, experimental scenarios are discussed which mimic constrained charged orbital motion. Experimental results illustrating the closed-loop regulator performance are presented.

COULOMB FORCE

A Coulomb force is generated by the interaction of two charged bodies. In space, this force is reduced by shielding from free-flying charged particles of the local plasma. The strength of this shielding is defined by the Debye length λ_d .¹⁹ The Coulomb force F_c that is generated between two craft of charges q_1 and q_2 is defined by

$$|F_c| = k_c \frac{q_1 q_2}{r^2} e^{-r/\lambda_d} \left(1 + \frac{r}{\lambda_d} \right) \quad (1)$$

where r is the spacecraft separation distance and $k_c = 8.99 \times 10^9 \text{ C}^{-2}\text{Nm}^2$ is the vacuum Coulomb constant. The Debye length is based on the temperature and density of the local plasma. At GEO the plasma is sufficiently hot and sparse to generate Debye lengths ranging from 80 -1000 m with an average of approximately 200 m,¹² allowing the use of Coulomb thrust when operating with spacecraft separations of dozens of meters at GEO. Low Earth orbit Debye lengths are typically cm level, making the use of Coulomb thrust challenging for feasible charge levels.

In the laboratory the spheres are operated in very close proximity where it is assumed there is no atmospheric interference or shielding and the generated Coulomb force can be modeled by the simple relationship

$$|F| = k_c \frac{q_1 q_2}{r^2} \quad (2)$$

where k_c here is the atmospheric Coulomb constant that is obtained by adjusting the vacuum constant with the relative permittivity of air. Testing indicates that there is some interaction of the charged spheres with the local laboratory atmosphere, in a similar nature to a spacecraft in its local plasma environment. Further investigation is required to understand and model this interaction and improve the accuracy of the atmospheric Coulomb force by modifying equation 2. For this study the simple Coulomb force relationship of equation 2 is used only as a reference for experimental results.

TESTBED HARDWARE APPARATUS

The preliminary developments of the testbed are described in detail in reference 18. This testbed setup has had some modifications and improvements to reach its present state used for the feedback control experiments detailed in this paper. Some of the most vital improvements are the reduction of disturbances as detailed in the following section.

As shown in figure 2 the testbed comprises a 1-D air bearing, all plastic track. It incorporates an autonomous air flow system using infrared (IR) sensors and valves to control the air to flow only underneath the cart. Polarity switching electrostatic power supplies, capable of $\pm 30 \text{ kV}$, are used to charge the aluminum spheres and control the motion of the cart. Each sphere has a diameter of 25 cm and the total cart mass is 0.5 kg. A laser is used for accurate external position sensing and is implemented in the feedback controller.

The whole apparatus sits on a glass table to limit external charge interference. The table is positioned inside a plastic cage for operational safety and is always operated with two personnel. The testbed now also features two LED systems. One is a warning light to indicate to operators that there is an active electrostatic charge from the power supplies and an array indicating the potential level. The second is an array of LEDs along the track length that align with each IR, valve, and air flow and signal the presence of the cart at that track location.

Custom hardware interface and GUI

The feedback control algorithm is implemented with the testbed hardware through a custom C-code application. The laser is interfaced through a serial port and distance measurements sampled at 50 Hz. The cart position is controlled by the spheres' charge which is driven by their respective voltage levels. The electrostatic power supplies are interfaced through a PCI express bus for analog output control and analog input status updates. A flowchart of the testbeds primary hardware systems and feedback implementation is shown in figure 3. The graphical user interface (GUI), shown in figure 4, allows the user to run the autonomous control scheme as well as any of the hardware systems manually and independently.

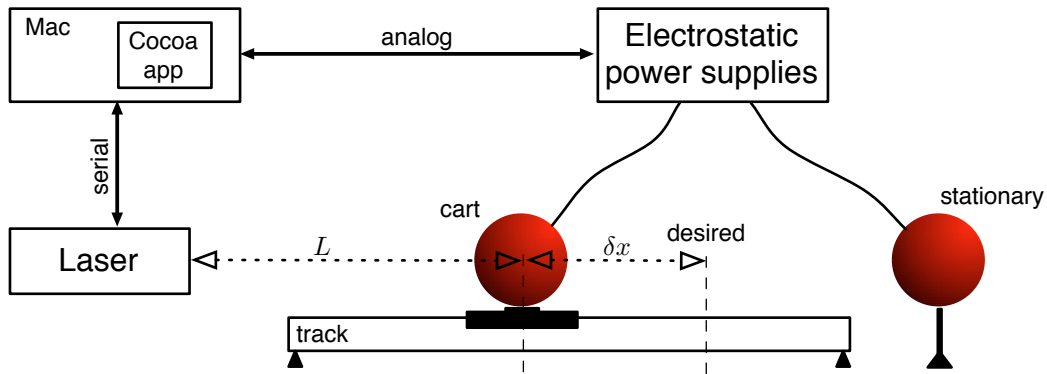


Figure 3. Flowchart of testbeds primary hardware systems and feedback implementation

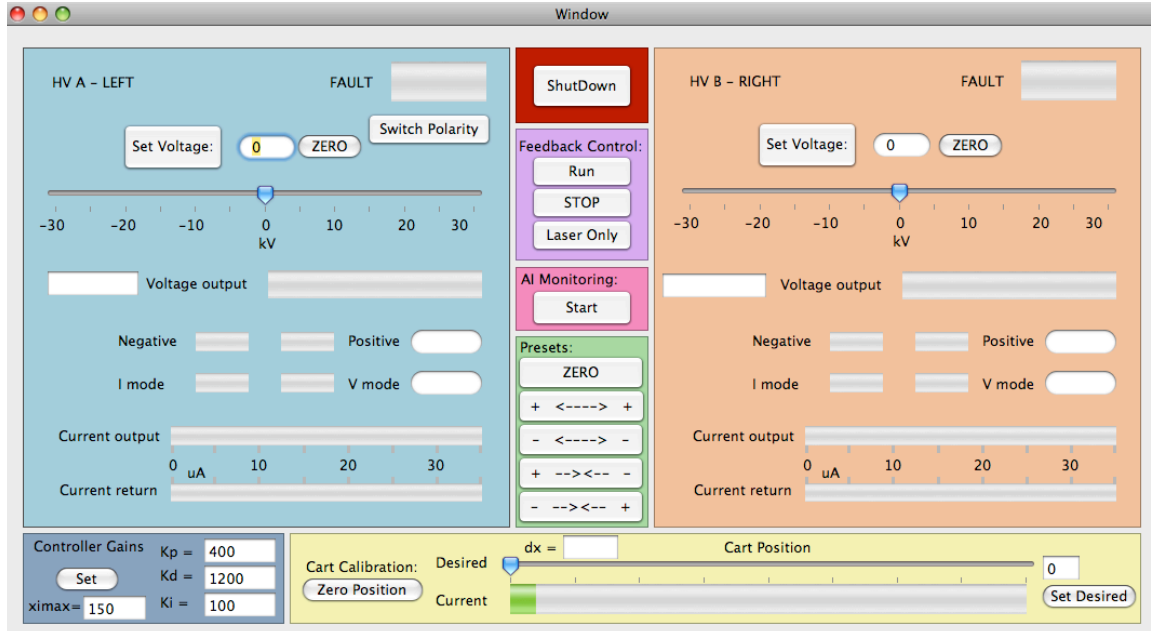


Figure 4. Custom graphical user interface for running the Coulomb testbed

DISTURBANCES

One of the greatest challenges to overcome with the Coulomb testbed is the mitigation of disturbances. It is necessary to reduce external disturbances to levels that give authority to the small Coulomb control forces. The previous Coulomb actuation experiments presented in reference 18 were performed on small sections of a track that had local variations causing gravity disturbances equivalent to 8.5 mN. Modifications to the current testbed track such as more regular airflow and a flatter track have greatly reduced gravitational and flow disturbances to around 1 mN over a 35 cm long section of track.

To further reduce disturbances, a new cart is developed for Coulomb controlled experiments. It is manufactured from polycarbonate for its smooth surface, dimensional stability and resistance to conduct and hold charge. Secondary effects of Coulomb applications, such as induced charge and sphere capacitance holding, are additional disturbances as initially highlighted in Reference 18. These effects are still present and are further discussed in the results section of this paper.

Another important consideration with the Coulomb testbed is maneuver durations. In space it is anticipated that Coulomb based maneuvers will be conducted on time scales of hours. Given that in the laboratory the disturbance force magnitudes are significantly greater relative to the control forces than expected in space, it is necessary to reduce the maneuver duration. All Coulomb motion experiments are conducted in durations of seconds to minutes. These testbed maneuvers are still a viable verification as they can be scaled to true orbit conditions.

Gravitational disturbances

Corrections to the track surface and leveling reduces the effects of gravitational disturbances. The testbed's plastic track encountered warping and cart velocity results indicate the introduction of disturbance gravity forces. The extent of the warping was on the order of 0.1° which resulted in a disturbance force as great as 8.5 mN for a 0.5 kg cart. It is desirable to reduce all disturbance forces below 2 mN, which for gravity disturbances corresponds to a track deviation angle less than 0.024° .

The track underwent resurfacing to remove the natural plastic warping and improve the surface flatness along its length. For rigidity and accuracy the track was machined in its constructed I-beam design in a unstressed state. Accurate measurements of the track surface indicate that the total variation along the track length is now less than 0.1 mm and a maximum angle deflection (measured at one end of the track) is 0.02° , resulting in a maximum gravity disturbance of 1.6 mN.

The current disturbances forces acting on the cart during glide tests are evident in figures 5 and 6. The cart's speed profile for a number of tests gliding toward the stationary sphere are shown in figure 5. These tests are conducted over the flat and level 35 cm track section with varying initial impulse speeds. Figure 6 shows a similar data set however the cart is traveling in the opposite direction away from the stationary sphere.

The slopes shown in figures 5 and 6 indicate a disturbance acceleration acting on the cart. With the 0.5 kg cart the average force is calculated to be 1.02 mN traveling toward the stationary sphere in figure 5 and 0.87 mN traveling away in figure 6. The acceleration is uniform across all initial speeds for both data sets. The cause for the cart accelerating in both directions is believed to be a combined consequence of the air flow and cart tilt (due to the high center of mass) while it is in motion. Research is currently underway to alleviate this problem, with methods such as lowering the carts center of gravity to below the center of pressure being investigated. Another contributing

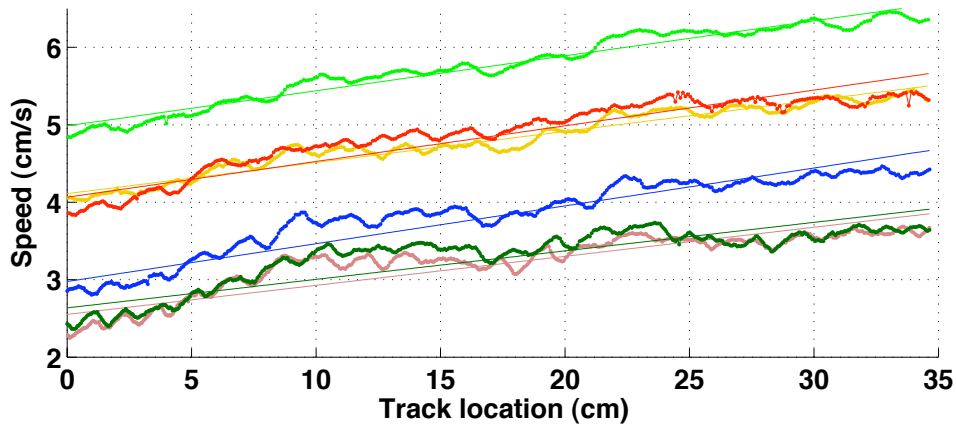


Figure 5. Cart glide data toward stationary sphere

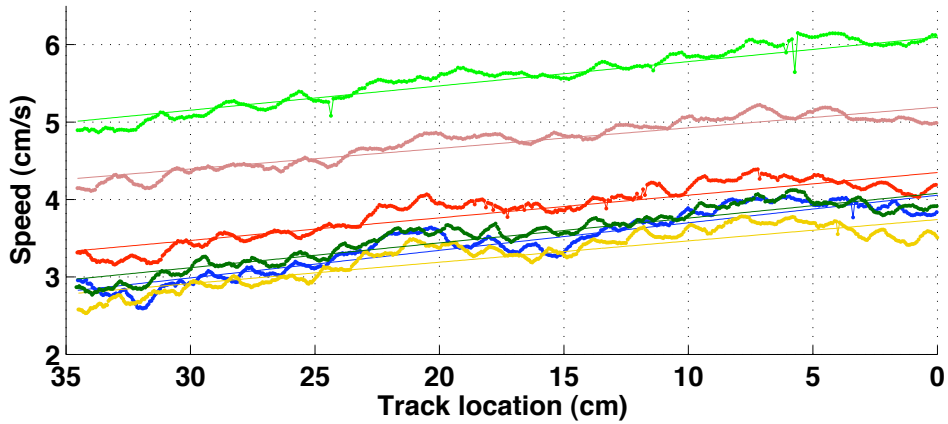


Figure 6. Cart glide data away from stationary sphere

factor to the cart experiencing a small acceleration in the direction of motion is due to the fact that the air flow to levitate the cart is only activated when the cart has triggered an infrared beam. Thus, while moving, the front section of the cart will always experience a reduced pressure compared to the rear section of the cart. This can cause a slight tilt and the measured forward acceleration.

This 35 cm flat and level section of track permits Coulomb controlled experiments to be conducted with disturbance forces around 1 mN. With a nominal stationary sphere location, the range of Coulomb control force achievable over this length of track is 3-18 mN with both repulsion and attraction. With these low disturbance forces in this separation range the cart motion is controllable with Coulomb forces. The Coulomb force is calculated using the simple relationship defined in equation 2 which does not model any atmospheric interactions or induced charges.

Air flow disturbances

Another disturbing force stems from the air flow supply along the track length. This force is due to uneven air flow between each row of air holes, which are controlled individually. There is also

potential disturbance contribution from inaccurate cart position sensing and the air valve switching on and off. To mitigate these errors the air supply at the track is carefully monitored with a highly accurate hot-wire air flow meter. This allows quantification of airflow inequalities along the track length, allowing them to be normalized with simple air flow regulation at each holes air supply.

To study and mitigate the effects of inaccurate cart positioning and the triggering of airflow, numerous glide tests are conducted with the cart, similar to that seen in figures 5 and 6. The tests vary the size and location of the IR reflective sheet. Prior to all Coulomb control experiments, glide tests with the cart and track configuration are conducted to ensure a minimum disturbance state is reached. An optimum configuration of minimum disturbance is selected and used for all Coulomb experiments conducted and presented in this paper.

CONSTRAINED RELATIVE MOTION DYNAMICS AND CONTROL

Significant knowledge is continuing to be developed regarding the theoretical aspects of the Coulomb thrust concept. Berryman and Schaub studied the use of Coulomb control to maintain static equilibrium configurations in orbit.^{20,21} This includes the analytic calculation of the Coulomb charges required to maintain static formations of two and three craft relative to a rotating Hill frame.²⁰ For the two craft system, the linear orientation can be paralleled to the charge control being achieved on the 1-D testbed. This work is also expanded to three dimensions with four craft equilibrium studies.²²

Equilibrium solutions for Coulomb controlled spacecraft are feasible, however stability is typically not guaranteed. To realistically implement the Coulomb thrust concept it is necessary to introduce feedback control. Reference 23 develops a control algorithm that stabilizes the motion of two craft about a orbit radial alignment while maintaining a fixed separation distance. Reference 24 details a restricted 1-D Lyapunov-based Coulomb control regime developed for three craft operating in a linear configuration. The intent of the testbed is to directly apply control algorithms such as these to Coulomb hardware. Reference 25 further develops the 1-D constrained control techniques to analyze the feasible regions of operation that can be implemented ensuring that the charge levels are realistic and do not saturate.

The studies of restricted 1-D linear relative motion control such as these could be implemented on the testbed apparatus. The algorithms use realistic Coulomb charges that are applied to the vehicle on the testbed. A vital step in the development of the Coulomb testbed is the implementation of position feedback control. A laser accurately senses the cart position to within a millimeter, which is input in real time to the controller of the electrostatic voltage supplies. This allows the relative cart position to be controlled to a desired location. The implementation and preliminary results of this position feedback control for relative motion are presented. These control experiments mimic 1-D constrained orbital motion in orbit radial, along-track and out-of-plane directions.

Testbed dynamical setup

The feedback control setup of the testbed with distance measurements from the laser is defined in figure 7. The laser measures the distance to the cart L , which corresponds to a distance x , from the stationary charged sphere. The desired position of the cart is defined by the distance x_r , which also defines the tracking control parameter δx .

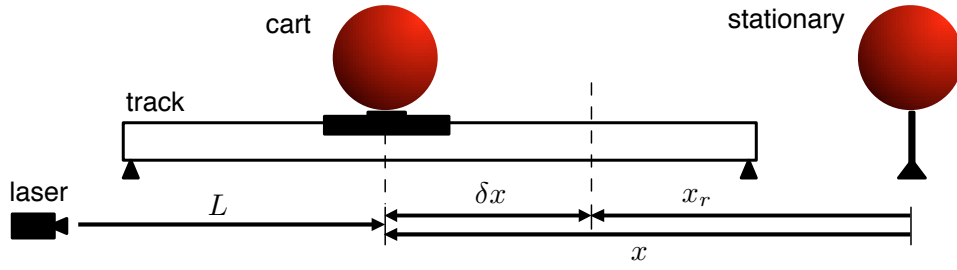


Figure 7. The testbed experimental variable setup

Using the Coulomb force from equation 2, the equation of motion for the cart on the track is defined by:

$$\ddot{x} = f(x, u, t) = \frac{1}{m} \left[\frac{k_c Q}{x^2} + f_{\text{system}} + f_{\text{unknown}} \right] \quad (3)$$

where Q is the combined charge product defined by $Q = q_1 q_2$, f_{system} represents known forces acting on the system (such as intentional gravity biases) and f_{unknown} are unmodeled disturbance forces. The cart motion is controlled through the combined charge product Q .

Orbit dynamical setup

The purpose of the testbed and this control methodology is not to simulate full orbital dynamic motions. Alternatively, restricted 1-D motions are feasible. It is possible to mimic 1-D constrained motion like the natural repulsive motion two spacecraft experience when separated in the orbit radial direction. Equations 4 show the linearized Clohessy-Wiltshire-Hill's equations²³ that can be used to develop a reference orbit. The equations define the motion of a satellite relative to a circularly orbiting reference point. The rotating Hill frame $\{\hat{o}_r, \hat{o}_\theta, \hat{o}_h\}$ has axis aligned in the orbit radial, along-track and out-of-plane directions respectively. The spacecraft position ρ_i is defined by the Cartesian x, y and z coordinates in this frame. Figure 8 shows the rotating Hill frame and example cases of two craft flying in the three potential operating configurations; orbit radial, along-track and out-of-plane.

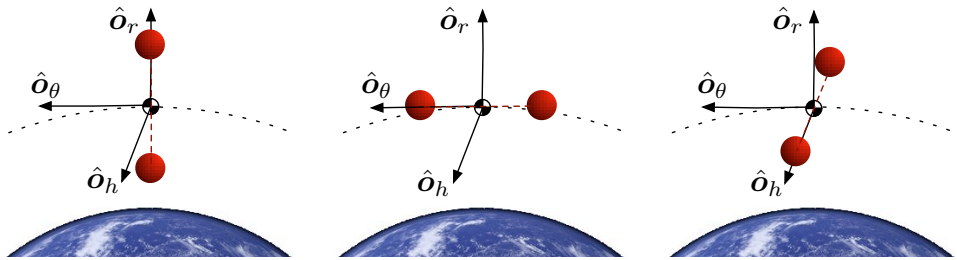


Figure 8 Two spacecraft example of the orbit radial, along-track and out-of-plane operating configurations in the rotating Hill frame.

With a formation of N Coulomb controlled spacecraft the CW-Hill equations of the i^{th} spacecraft relative to the orbit reference is defined by²³

$$\ddot{x}_i - 2\Omega\dot{y}_i - 3\Omega^2x_i = \frac{k_c}{m_i} \sum_{j=1, j \neq i}^N \frac{(x_i - x_j)}{|\boldsymbol{\rho}_i - \boldsymbol{\rho}_j|^3} q_i q_j e^{-r_{12}/\lambda_d} \left(1 + \frac{r_{12}}{\lambda_d}\right) \quad (4a)$$

$$\ddot{y}_i + 2\Omega\dot{x}_i - 3\Omega^2x_i = \frac{k_c}{m_i} \sum_{j=1, j \neq i}^N \frac{(y_i - y_j)}{|\boldsymbol{\rho}_i - \boldsymbol{\rho}_j|^3} q_i q_j e^{-r_{12}/\lambda_d} \left(1 + \frac{r_{12}}{\lambda_d}\right) \quad (4b)$$

$$\ddot{z}_i + \Omega^2z_i = \frac{k_c}{m_i} \sum_{j=1, j \neq i}^N \frac{(z_i - z_j)}{|\boldsymbol{\rho}_i - \boldsymbol{\rho}_j|^3} q_i q_j e^{-r_{12}/\lambda_d} \left(1 + \frac{r_{12}}{\lambda_d}\right) \quad (4c)$$

where the orbital rate of the reference point (r_c) is defined as $\Omega = \sqrt{GM_e/r_c^3}$, where G is the gravitational constant, M_e is the Earth's mass and m_i is each spacecraft's mass. These equations can be constrained to 1-D motion along the orbit radial, along-track and out-of-plane directions. With only two craft in the formation and ignoring any plasma Debye shielding the 1-D relative equations of motion become:

$$\ddot{x}_i - 3\Omega^2x_i = \frac{k_c}{m_i} \frac{Q}{(x_i - x_j)^2} \quad (5a)$$

$$\ddot{y}_i = \frac{k_c}{m_i} \frac{Q}{(y_i - y_j)^2} \quad (5b)$$

$$\ddot{z}_i + \Omega^2z_i = \frac{k_c}{m_i} \frac{Q}{(z_i - z_j)^2} \quad (5c)$$

Analyzing the orbit radial direction, there is an equilibrium condition where x_i is held constant with charges $Q < 0$.²⁰ The natural repulsion force (gravity gradient) experienced by the spacecraft indicates a mixed charged (attractive) Coulomb force is necessary to maintain relative separation equilibria. This restricted operating scenario is mimicked with the craft on the testbed. Using an inclined track a natural gravitation bias force is introduced to the system. The constant repulsive gravity force is similar to the linearly dependent gravity gradient of equation 5a and can be overcome with Coulomb forces to drive and hold the cart to a desired separation distance.

Similarly, the out-of-plane direction (equation 5c) contains equilibria with constant z_i when $Q > 0$,²⁰ hence, a repulsive Coulomb force is needed. This configuration is comparable to experiments on the testbed with a inclined track toward the stationary charged node. The constant attractive gravity bias is similar to the linearly dependent gravity gradient of equation 5c.

The Hill frame along-track direction (equation 5b) is neutral and requires $Q = 0$ to maintain a fixed y_i coordinate separation. This condition is simulated on the testbed with a level track and no bias forces. Of these three simulations, the along-track direction is the most challenging to implement because of the need to have a flat and level track and to minimize all disturbances. The orbit radial and normal direction simulations are easier to implement since any track un-level biases can be exploited to provide slight gravitation pull or repulsion to simulate this charged axial orbital motion.

The testbed results of implementing feedback control with these three orbit-similar configurations are presented in the paper. In order to achieve the described two spacecraft, orbit-similar scenarios,

it is necessary to have the setup where one sphere is stationary as shown in figure 7. Further studies will incorporate multiple craft on the track and ultimately expand to 2-D motion studies.

Control law

The control parameter of the testbed system is the combined charge product Q . A PID controller is implemented to control the system with position feedback, introduce damping to the system response and account for any unmodeled disturbance forces. With the system of equation 3 linearized about a equilibrium position a control law is defined as:

$$u = -k_D\delta\dot{x} - k_P\delta x - k_I \int_0^t \delta x dt - f_{\text{system}} = \frac{k_c Q}{x^2} \quad (6)$$

where k_P , k_D , and k_I are controller gains. This non-linear charge feedback control law Q features feedforward compensation when known biases f_{system} are acting on the hovering cart. The integral feedback adds robustness to the system to account for discrepancies in modeling of f_{system} and the limited model of charge interaction with the atmosphere. Future models of electrostatic interaction with the atmosphere could be added to this control law. Substituting the control law into the linearized equation of motion results in the following closed loop dynamics:

$$\delta\ddot{x} + k_D\delta\dot{x} + k_P\delta x + k_I \int_0^t \delta x dt = 0 \quad (7)$$

With positive control gain values the feedback linearized system response is stable.

Numerical simulations

The cart motion under the proposed position feedback algorithm is simulated using the Coulomb force and control defined in equation 6. For sloped track experiments mimicking a 1-D relative orbit bias, a constant force is added to the model through the f_{system} term. System performance and stability analysis of the controller is simulated on this model prior to implementation on the testbed.

A simulation of a cart's motion and required control parameters is shown in figure 9. This simulation begins with a cart initially at rest with a separation of 30 cm (center to center). The cart is then accelerated and controlled on a downward slope with a constant gravity bias force of 2 mN and controlled to a distance 30 cm away.

The first plot of the figure shows the distance of the cart away from the desired location in centimeters. The response of the cart has little overshoot and has a 5% settling time of 23 seconds. This is suitable for the control of the cart on the testbed and is controllable with feasible voltages as shown in the second plot of the figure which shows saturation only for the initial second. This cart control within seconds is much faster than anticipated for the control of spacecraft in orbit which is expected to take hours to perform similar scaled maneuvers.

The second plot of the figure shows the voltage of both the cart (A) and the stationary sphere (B). Initially the cart is repelled away but the voltage quickly changes to opposing polarity, producing an attractive force that prevents the cart from sliding down the simulated sloped track. The steady state voltage is ≈ 20 kV which provides a 2 mN force at that separation distance as shown in the lower plot of figure 9.

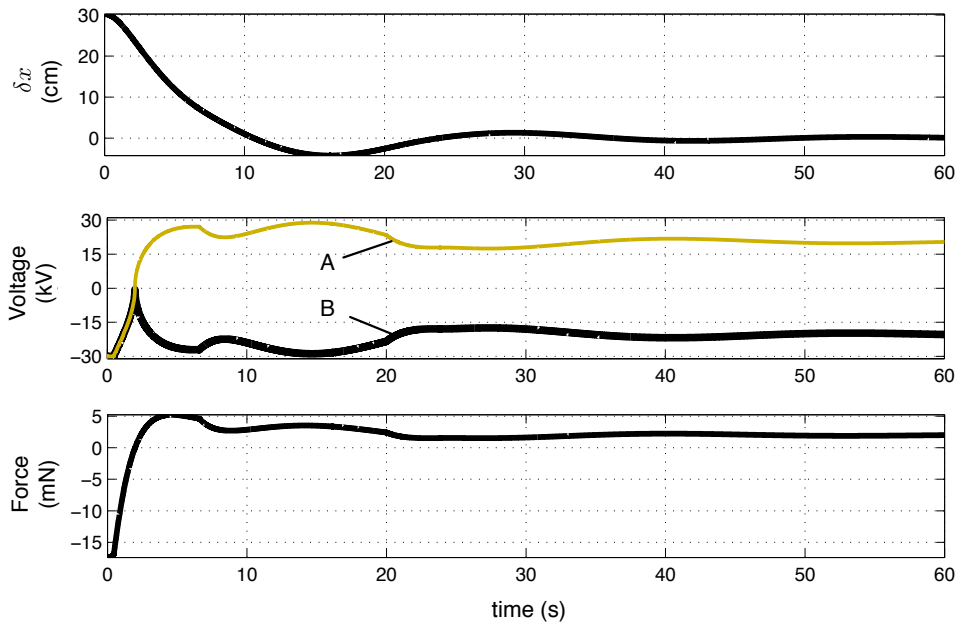


Figure 9. Simulation of cart motion with a constant system force of 2 mN

POSITION CONTROL EXPERIMENTAL RESULTS

The cart motion is controlled using Coulomb forces on a flat and level track as well as an inclined track. A inclined track simulates an operating environment with a fixed bias acceleration acting on the craft, such as that experienced in a simplified orbit radial (relative repulsive acceleration) or orbit normal (relative attractive acceleration). The results of the testing are presented here.

Control results on a flat and level track: along-track configuration

The Coulomb control algorithm is first implemented on a flat and level track. The track is leveled using both precision level instruments and verified via glide experiments with the test cart. All glide tests indicate a slight acceleration of 1-2 mN in the direction of motion as shown in figures 5 and 6. Regardless, the Coulomb experiments are conducted here with a cart that stands motionless on the sections of track tested.

Figure 10 displays the cart motion and control parameters required to drive the cart a total of 30 cm. The cart starts from rests and repels from an initial separation of 30 cm (center to center) from the stationary sphere. The cart δx is shown in the top plot for two identical tests. A magnification showing the settlement of the cart at the desired location is also shown for each test. The center plot shows the voltage levels that are used to control the cart during test 1 for both the cart sphere (A) and the stationary sphere (B). When the voltage magnitudes are equivalent magnitude the Coulomb force is repulsive, with mixed magnitudes the force is attractive. By design the spheres are sent to a negative potentials when repulsive forces are required. The lower figure shows the Coulomb force acting on the cart in test 1 using the relationship defined in equation 2.

The results shown in Figure 10 indicate that the cart can be controlled on a level track to a desired position using Coulomb forces. The cart motion, δx , shows that the system has a 5% settling time of 19 s and a 1% settling time of 34 s for test 2 and 39 s for test 1. These settling times are similar

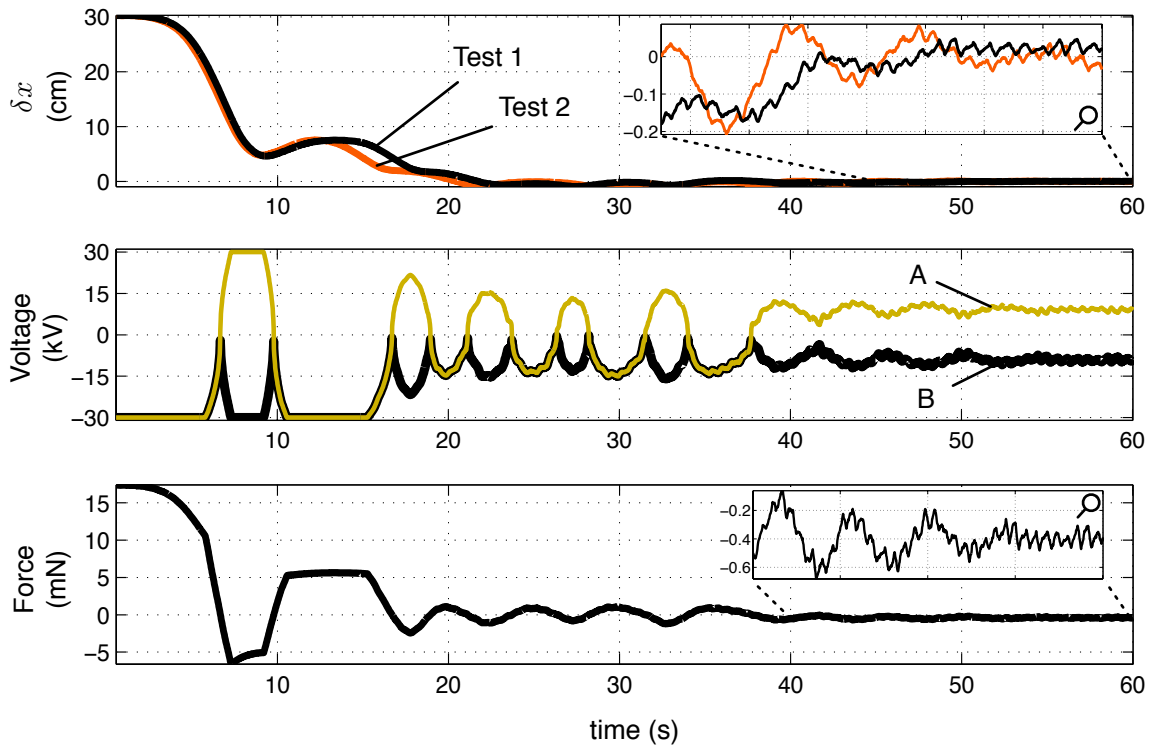


Figure 10 Cart control on flat and level track that mimics a two craft, along track orbit configuration

to that anticipated for a cart on a level track. The cart is within 1 mm of the desired location within 45 seconds of the tests duration.

A deviation from the simulation results is the increased oscillations or under-damped nature that appears with the hardware results. This is magnified with the voltage levels required to control the cart, even with the damping gain being enhanced for this test. For a level track it is anticipated that the control voltage is zero, however the steady state voltage is ± 9 kV. It is found that when the voltage is removed the cart will remain stationary at that spot indicating there is no gravity acting. At this separation distance and steady state voltage the resulting attractive Coulomb force is (≈ 0.4 mN). This source of this disturbance force is unknown, however it is likely a result of electrostatic interaction of the spheres with the atmospheric environment in the lab or secondary induced effects.

Inclined track results: orbit radial configuration

With position feedback control successfully implemented on the 1-D level track, the track is intentionally inclined sloping down from the stationary sphere. Using this position feedback control technique the craft is held at a fixed separation distance on the inclined track by holding a constant attractive charge (mixed polarity voltage). Figure 11 displays the cart motion and control parameters required to drive the cart a total of 28 cm. The cart starts from rests and repels from a initial separation of 30 cm (center to center) from the stationary sphere.

The results in figure 11 show a similar response to the cart motion for a level track. The 5% settling time of the cart is ≈ 25 s with a 1% settling time of 43 s for test 1 and 47 s for test 2. Once again, these settling times are very similar to the anticipated simulation results shown in figure 9.

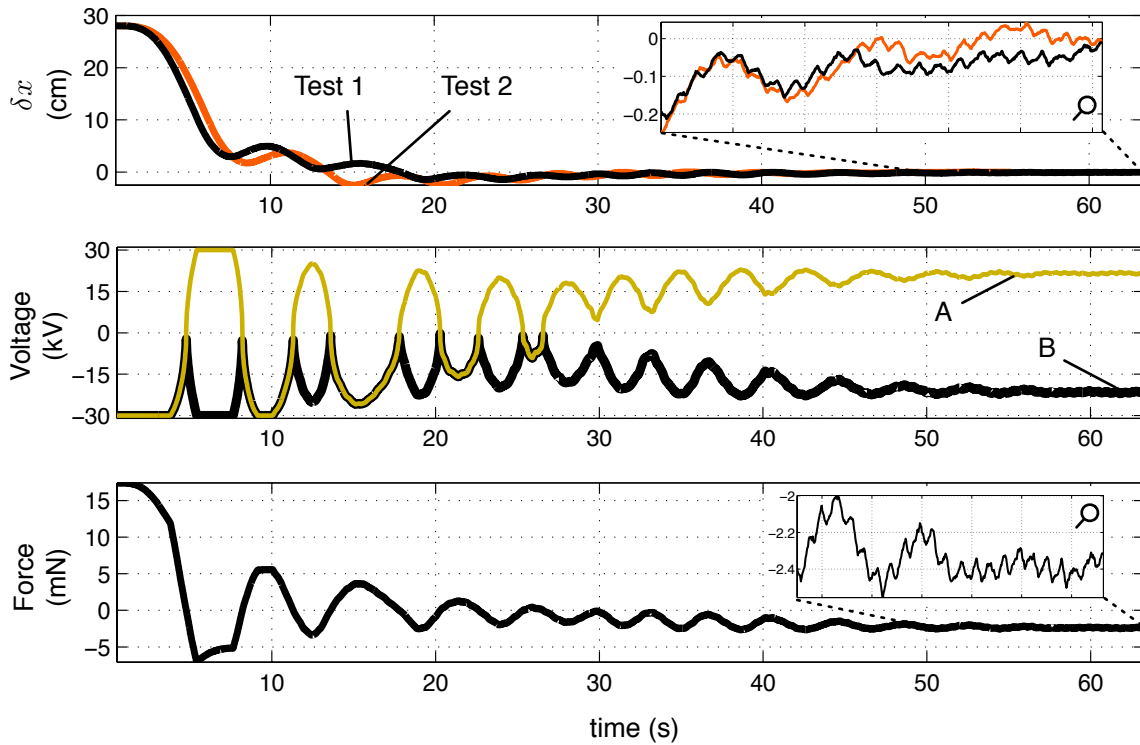


Figure 11. Cart control on inclined track that mimics a two craft, orbit radial configuration

The cart is within 1 mm of the desired location by 55 seconds into the tests. As before the testbed demonstrated less damping than anticipated with the simulations.

The voltage levels required to drive the cart to steady state shows the elevated results for the level track as anticipated. The steady state voltage level is ± 21.5 kV. Also shown in figure 11 is the steady state voltage level which results in a attractive Coulomb force ≈ 2.4 mN at this separation distance. With the voltage removed the cart will accelerate away from the stationary sphere. Glide tests performed immediately after the Coulomb tests indicate the acceleration from this location to be ≈ 4.5 mN. There reasons for this discrepancy could be electrostatic interferences that were measured with the previous level track experiments, as well as the extra acceleration terms that are measured once the cart is in motion.

These results are comparable in magnitude with what is required for a two craft system operating in a radial configuration in GEO. The differential radial gravitational force magnitude linearizes to¹²

$$\delta F_r \approx m \frac{3\mu}{r_c^3} L \quad (8)$$

where m is the spacecraft mass, μ is the gravitational constant, r_c is the system center of mass orbit radius and L is the spacecraft separation distance. Consider two spacecraft each with a mass of 50 kg and a separation of 20 m aligned in the radial direction. At GEO the gravity gradient force is $\approx 16 \mu\text{N}$. To overcome this force with Coulomb control requires a charge of $0.84 \mu\text{C}$, in a plasma with a Debye length of 200 m. This corresponds to required voltage magnitudes of 15.2 kV if each craft were assumed spherical with a radius of 0.5 m. This testbed experiment shows an application that mimics a potentially realistic orbital configuration. One thing to consider, is that the experiment

is conducted on a much shorter time scale than what is anticipated in an orbit application that may take hours to perform a similar maneuver.

Inclined track results: out-of-plane configuration

For the final series of experiments the track is intentionally inclined sloping upward away from the stationary sphere. Using the position feedback control technique the craft is held at a fixed separation distance on the inclined track by holding a constant repulsive charge (equivalent polarity voltage). Two separate configurations are examined. The first starts with a cart at rest at a separation of 30 cm (center to center) from the stationary sphere and ascends the track. Figure 12 displays the cart motion and control parameters required to drive the cart up the slope a total of 11 cm.

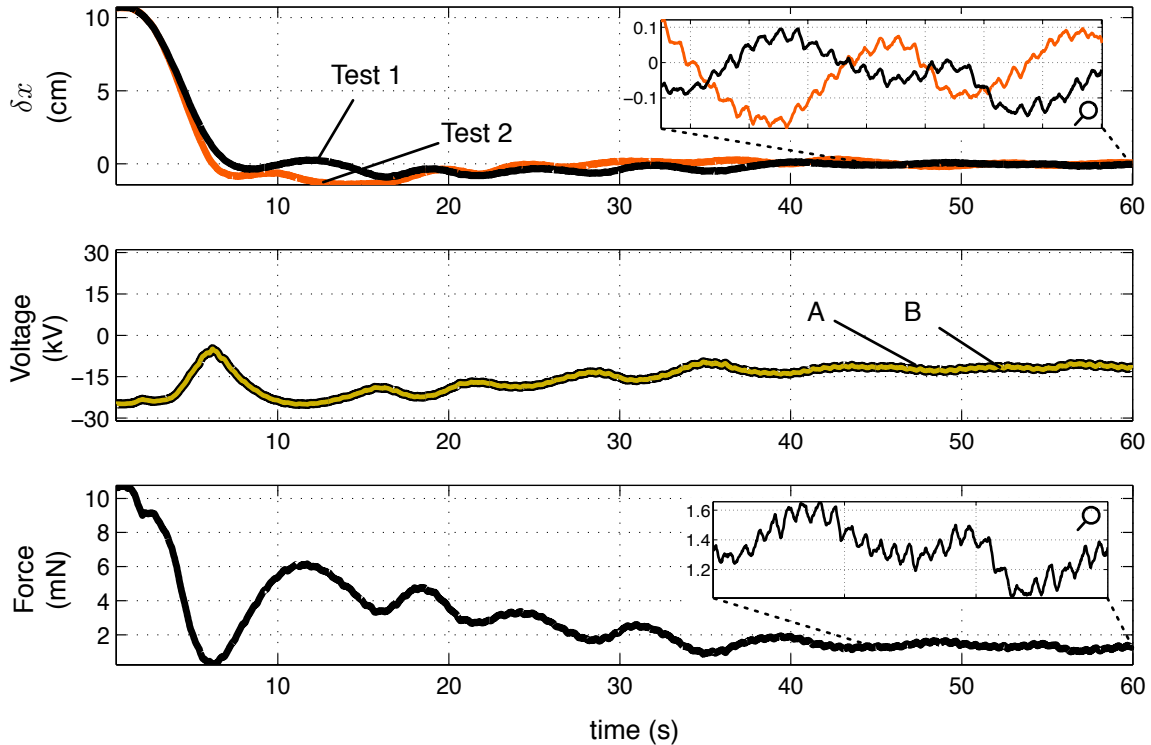


Figure 12 Cart control on inclined track that mimics a two craft, out-of-plane configuration : (starts down slope)

This test indicates that the cart is driven to the desired location with little or no overshoot as it is maneuvered up the slope. The cart settles to ± 1 mm of the target location with a 5% settling time of ≈ 23 seconds, which is comparable to simulations. The Coulomb force required to drive the cart this distance remains repulsive. The resulting voltage to maintain the cart at this location is ≈ -12 kV which equates to a force of ≈ 1.3 mN, calculated using equation 2 relationship.

The second orbit normal tests start with the cart at rest away from the sphere and descending to the desired position. The cart is initially separated by 72 cm (center to center) and driven 30 cm down slope toward the sphere. As shown in figure 13, the down slope momentum of the cart causes a larger overshoot in this case, but the controller drives the cart to within ± 2 mm of desired. The 5% settling time is 24 s for test 1 and 28 s for test 2. The steady state voltage is ≈ -15 kV which equates to a force of ≈ 2.3 mN, calculated using equation 2 relationship. Using glide test

data collected after this experiment it is found that the acceleration due to gravity at this location is ≈ 2 mN. This agrees well with the assumed Coulomb force (calculated with the relationship of equation 2) required to overcome this bias force.

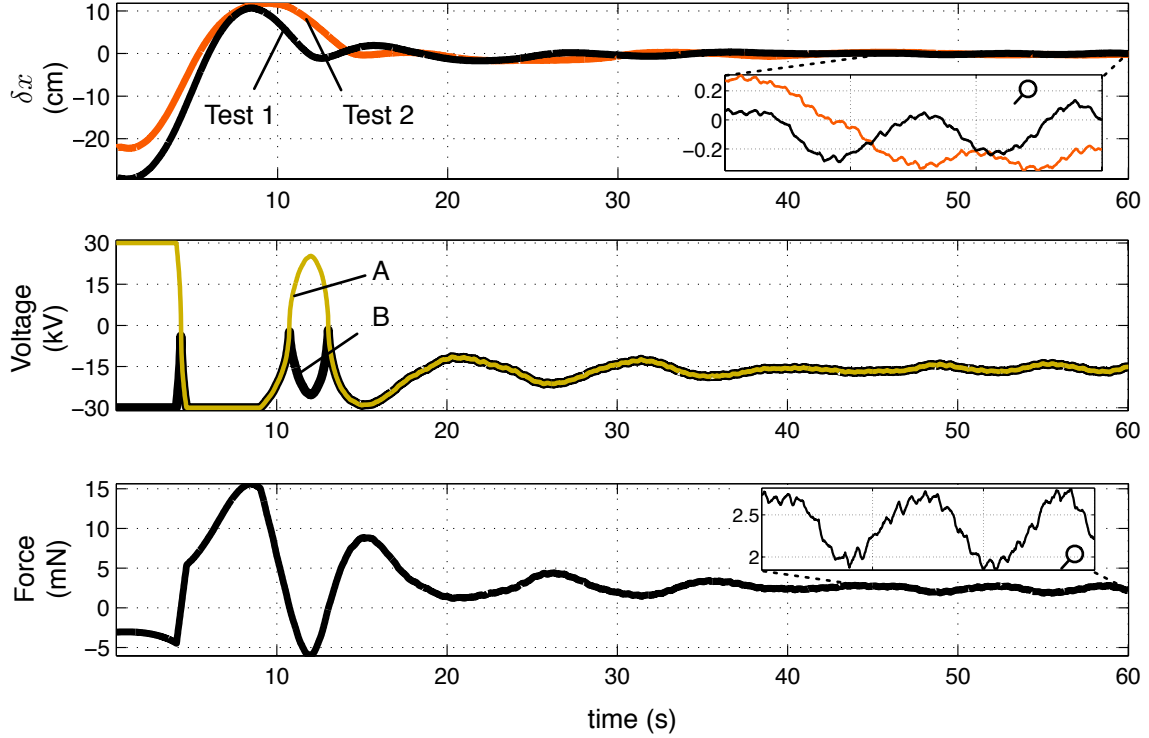


Figure 13 Cart control on inclined track that mimics a two craft, out-of-plane configuration : (starts up slope)

It is noted with these orbit normal similar operating scenarios that the steady state conditions experience greater oscillations than the previous experiments. A cause of this may be electrostatic interference with the atmosphere that has been witnessed when conducting equivalent polarity experiments. This is the reason the experiments are conducted with the desired location being much closer to the stationary sphere to allow the cart to come to a controllable rest.

The orbit normal similar results shown here resemble what could be used by a two craft system operating in a orbit normal configuration in GEO. The differential orbit normal gravitational force magnitude linearizes to¹²

$$\delta F_h \approx m \frac{\mu}{r_c^3} L \quad (9)$$

Now consider the equivalent spacecraft of the previous example, separated by 20 m in the orbit normal direction. The attractive force experienced is $\approx 5.3 \mu\text{N}$. To overcome this force with Coulomb control requires a charge of $0.49 \mu\text{C}$, corresponding to a spacecraft voltage of 8.8 kV. Once again this experiment is conducted on a much smaller timescale than what is anticipated in a orbit application that may take hours to perform a similar, yet scaled maneuver.

CONCLUSIONS

This paper documents the developments of the Coulomb testbed and presents feedback control results. This includes the details of quantifying and significantly reducing disturbance forces that consequently improves the Coulomb actuation capabilities of the testbed.

A new and exciting feature and major focus of this paper is the implementation of position feedback control. This is an important step in the development of the Coulomb control concept. The results of controlling the position of a single cart relative to a fixed charged node is presented. The control is implemented on a flat and level track as well as an inclined track that adds a gravitational bias to the cart's motion. These experiments are similar in nature to the restricted 1-D motion that is experienced by two craft flying in a close orbit formation.

These successful autonomous position feedback control results open countless opportunities for the Coulomb testbed. The implementation of more advanced control algorithms and multiple craft are in planning. The ultimate goal is to apply the techniques to multiple craft moving independently on the track and control their relative separation distance and evolve to a two-dimensional testbed.

REFERENCES

- [1] J. Leitner, F. Bauer, J. How, M. Moreau, R. Carpenter, and D. Folta, "Formation Flight in Space: Distributed Spacecraft Systems Develop New GPS Capabilities," *GPS World*, February 1 2002.
- [2] J. R. Carpenter, J. A. Leitner, D. C. Folta, and R. D. Burns, "Benchmark Problems for Spacecraft Formation Flying Missions," *AIAA Guidance, Navigation and Control Conference*, Austin, TX, August 11–14 2003. Paper No. AIAA 2003-5364.
- [3] L. B. King, G. G. Parker, S. Deshmukh, and J.-H. Chong, "Spacecraft Formation-Flying using Inter-Vehicle Coulomb Forces," tech. rep., NASA/NIAC, January 2002. <http://www.niac.usra.edu>.
- [4] L. B. King, G. G. Parker, S. Deshmukh, and J.-H. Chong, "Study of Interspacecraft Coulomb Forces and Implications for Formation Flying," *AIAA Journal of Propulsion and Power*, Vol. 19, May–June 2003, pp. 497–505.
- [5] E. G. Mullen, M. S. Gussenhoven, D. A. Hardy, T. A. Aggson, and B. G. Ledley, "SCATHA Survey of High-Voltage Spacecraft Charging in Sunlight," *Journal of the Geophysical Sciences*, Vol. 91, No. A2, 1986, pp. 1474–1490.
- [6] E. C. Whipple and R. C. Olsen, "Importance of differential charging for controlling both natural and induced vehicle potentials on ATS-5 and ATS-6," *Proceedings of the 3rd Spacecraft Charging Technology Conference*, Nov. 12–14 1980, p. 887. NASA Conference Publication 2182.
- [7] E. Mullen, A. R. Frederickson, G. P. Murphy, K. P. Ray, E. G. Holeman, D. Delorey, R. Robson, and M. Farar, "An Autonomous Charge Control System at Geosynchronous Altitude: Flight Results for Spacecraft Design Considerations," *IEEE Transactions on Nuclear Science*, Vol. 44, December 1997, pp. 2188 – 2914.
- [8] J. F. Fennell, H. C. Koons, J. L. Roeder, and J. B. Blake, "Spacecraft Charging: Observations and Relationship to Satellite Anomalies," *Proceedings of 7th Spacecraft Charging Technology Conference*, Noordwijk, The Netherlands, ESA Spec. Publ., April 23–27 2001.
- [9] H. B. Garrett and A. C. Whittlesey, "Spacecraft Charging, An Update," *IEEE Transactions on Plasma Science*, Vol. 28, Dec. 2000, pp. 2017–2028.
- [10] K. Torkar and et. al., "Spacecraft Potential Control aboard Equator-S as a Test for Cluster-II," *Annales Geophysicae*, Vol. 17, 1999, pp. 1582–1591.
- [11] K. Torkar, W. Riedler, and et. al., "Active Spacecraft Potential Control for Cluster – Implementation and First Results," *Annales Geophysicae*, Vol. 19, No. 10/12, 2001, pp. 1289–1302.
- [12] C. R. Seubert and H. Schaub, "Tethered Coulomb Structures: Prospects and Challenges," *AAS F. Landis Markley Astrodynamics Symposium*, Cambridge, MA, June 30 – July 2 2008. Paper AAS 08–269.
- [13] K. G. Carpenter, C. J. Schrijver, M. Karovska, and S. M. C. D. Team, "The Stellar Imager (SI) Project: A Deep Space UV/Optical Interferometer (UVOI) to Observe the Universe at 0.1 Milli-arcsec Angular Resolution," *Proceedings of the NUVA Conference*, El Escorial, Spain, June 2007.
- [14] G. Blackwood, C. Henry, E. Serabyn, S. Dubovitsky, M. Aung, and S. M. Gunter, "Technology and Design of an Infrared Interferometer for the Terrestrial Planet Finder," *AIAA Space 2003*, Long Beach, CA, Sept. 23–25 2003. Paper No. AIAA 2003-6329.

- [15] N. Murdoch, D. Izzo, C. Bombardelli, I. Carnelli, A. Hilgers, and D. Rodgers, "Electrostatic Tractor for Near Earth Object Deflection," *59th International Astronautical Congress*, Glasgow, Scotland, 2008. Paper IAC-08-A3.I.5.
- [16] D. P. Scharf, F. Y. Hadaegh, J. A. Keim, A. C. Morfopoulos, A. Ahmed, Y. Brenman, A. Vafaei, J. F. Shields, C. F. Bergh, and P. R. Lawson, "Flight-like Ground Demonstrations of Precision Maeuvers for Spacecraft Formations," *AIAA Guidance, Navigation and Control Conference*, Honolulu, Hawaii, Aug. 18–21 2008. Paper No. AIAA 2008-6665.
- [17] S.-J. Chung, D. Adams, D. W. Miller, E. Lorenzini, and D. Leisawitz, "SPHERES Tethered Formation Flight Testbed: Advancements in Enabling NASA's SPECS Mission," *SPIE – Proceedings of Astronomical Telescopes and Instrumentation 2006 Conference*, 2006. Paper 6268-11.
- [18] C. R. Seubert and H. Schaub, "One-Dimensional Testbed for Coulomb Controlled Spacecraft," *AAS/AIAA Spaceflight Mechanics Meeting*, Savannah, GA, Feb. 8–12 2009. Paper AAS 09–015.
- [19] T. I. Gombosi, *Physics of the Space Environment*. New York, NY: Cambridge University Press, 1998.
- [20] J. Berryman and H. Schaub, "Analytical Charge Analysis for 2- and 3-Craft Coulomb Formations," *AIAA Journal of Guidance, Control, and Dynamics*, Vol. 30, Nov.–Dec. 2007, pp. 1701–1710.
- [21] J. Berryman and H. Schaub, "Static Equilibrium Configurations in GEO Coulomb Spacecraft Formations," *AAS/AIAA Spaceflight Mechanics Meeting*, Copper Mountain, CO, Jan. 23–27 2005. Paper No. AAS 05–104.
- [22] H. Vasavada and H. Schaub, "Analytic Solutions for Equal Mass Four-Craft Static Coulomb Formation," *AAS/AIAA Astrodynamics Specialist Conference*, Mackinac Island, MI, Aug. 19–23 2007. Paper AAS 07–268.
- [23] A. Natarajan and H. Schaub, "Linear Dynamics and Stability Analysis of a Coulomb Tether Formation," *AIAA Journal of Guidance, Control, and Dynamics*, Vol. 29, July–Aug. 2006, pp. 831–839.
- [24] S. Wang and H. Schaub, "One-Dimensional 3-Craft Coulomb Structure Control," *7th International Conference on Dynamics and Control of Systems and Structures in Space*, Greenwich, London, England, July 16–20 2006, pp. 269–278.
- [25] S. Wang and H. Schaub, "1-D Constrained Coulomb Structure Stabilization With Charge Saturation," *AAS/AIAA Astrodynamics Specialist Conference*, Mackinac Island, MI, Aug. 19–23 2007. Paper AAS 07–267.